Role of the Hydrogen Bond from Leu722 to the A_{1A} Phylloquinone in Photosystem I[†,‡]

Nithya Srinivasan,[§] Irina Karyagina,[||] Robert Bittl,[||] Art van der Est,[⊥] and John H. Golbeck*[,§,#]

Department of Biochemistry and Molecular Biology, The Pennsylvania State University, University Park, Pennsylvania 16802, Institut für Experimental Physik, Fachbereich Physik, Freie Universität Berlin, Arnimallee 14, D14195 Berlin, Germany, Department of Chemistry, Brock University, 500 Glenridge Avenue, St. Catharines, ON L2S 3A1, Canada, and Department of Chemistry, The Pennsylvania State University, University Park, Pennsylvania 16802

Received December 22, 2008; Revised Manuscript Received February 27, 2009

ABSTRACT: Photosystem I (PS I) contains two molecules of phylloquinone that function as electron transfer cofactors at highly reducing midpoint potentials. It is therefore surprising that each phylloquinone is hydrogen bonded at the C_4 position to the backbone −NH of a Leu residue since this serves to drive the midpoint potential more oxidizing. To better understand the role of the H-bond, a PS I variant was generated in which $L722_{PsaA}$ was replaced with a bulky Trp residue. This change was designed to alter the conformation of the A-jk(1) loop and therefore change the strength of the H-bond to the PsaA-branch phylloquinone. Transient EPR studies at 80 K show that the A_{1A} site in the PS I variant is fully occupied with phylloquinone, but the absence of methyl hyperfine couplings in the quinone contribution to the $P_{700}^{\bullet+}A_1^{\bullet-}$ radical pair spectrum indicates that the H-bond has been weakened. In wild-type PS I, reduction of F_A and F_B with sodium dithionite causes a ∼30% increase in the amplitude of the $P_{700}^{\bullet+}A_1^{\bullet-}$ transient EPR signal due to the added contribution of the PsaB-branch cofactors to low temperature reversible electron transfer between P_{700} and A_{1A}. In contrast, the same treatment to the $L722W_{PsaA}$ variant leads to a ∼75% reduction in the amplitude of the $P_{700}^{\bullet+}A_1^{\bullet-}$ transient EPR signal. This behavior suggests that A_{1A} has undergone double reduction to phyllohydroquinone, thereby preventing electron transfer past A_{0A}. The remaining 25% of the $P_{700}^{\bullet+}A_1^{\bullet-}$ radical pair spectrum shows an altered spin polarization pattern and pronounced methyl hyperfine couplings characteristic of asymmetric H-bonding to the phylloquinone. Numerical simulations of the polarization pattern indicate that it arises primarily from electron transfer between P_{700} and A_{1B}. The altered reduction behavior in the $L722W_{PsaA}$ variant suggests that the primary purpose of the H-bond is to tie up the C_4 carbonyl group of phylloquinone in a H-bond so as to prevent protonation and hence lower the probability of double reduction during periods of high light intensity.

Photosynthetic reaction centers are classified as one of two types depending on the cofactor which functions as the terminal electron acceptor. Type I reaction centers employ a bound iron−sulfur cluster, while type II reaction centers employ a mobile quinone. The underlying common structural motif of both type I and type II reaction centers includes the presence of a protein dimer that forms the photoactive core, anchoring the two branches of electron transfer cofactors that span the width of the membrane (*1*). In oxygenic photosynthetic organisms, the type I reaction center is Photosystem I (PS I)[1] and its photoactive core is composed of a heterodimer of the PsaA and PsaB proteins (*2*). The electron transfer chain begins at the primary electron donor, P_{700}, which is a special pair of Chl *a*/*a*′ molecules ligated by PsaB and PsaA, respectively (*3*). The chain bifurcates into two branches (denoted by the A and B subscripts according to the protein subunits), each consisting of two additional Chl *a* molecules, A_{-1A} and A_{0A} (A_{-1B} and A_{0B}), and one phylloquinone molecule, A_{1A} (A_{1B}). The chain reconverges at the [4Fe-4S] cluster F_X, which is ligated by four cysteine residues, two of which are provided by PsaA and two of which are provided by PsaB. Two additional [4Fe-4S] clusters, labeled F_A and F_B, are bound to the stromal PsaC protein and function in series to accept the electron from F_X and transfer it to soluble ferredoxin.

There is now a convincing body of evidence that points toward bidirectional electron transfer in plant, algal, and cyanobacterial PS I, although the extent to which the two branches are active is still under investigation (*4*−*9*). Below the glass transition temperature, two distinct fractions are formed such that irreversible charge separation to F_A/F_B occurs in one fraction and reversible electron transfer between P_{700} and A_1 occurs in the other (*10*). It has been

[†] This work was supported by a grant from the National Science Foundation (MCB-0519743) to J.H.G., by Deutsche Forschungsgemeinschaft Grant SFB 498 to R.B. and by NSERC to A.v.d.E.

[‡] This paper is dedicated to the memory of Dietmar Stehlik (born May 1939, died August 2007).

* To whom correspondence should be addressed. Tel: 1 814 865 1163. Fax: 1 814 863 7024. E-mail: jhg5@psu.edu.

[§] Department of Biochemistry and Molecular Biology, The Pennsylvania State University.

[||] Freie Universität Berlin.

[⊥] Brock University.

[#] Department of Chemistry, The Pennsylvania State University.

[1] Abbreviations: PS I, Photosystem I; CW, continuous wave; EPR, electron paramagnetic resonance; ENDOR, electron nuclear double resonsonance; HEPES, *N*-2-hydroxyethylpiperazine-*N*′-2-ethanesulfonic acid; Chl, chlorophyll.

10.1021/bi802340s CCC: $40.75
Published on Web 03/01/2009

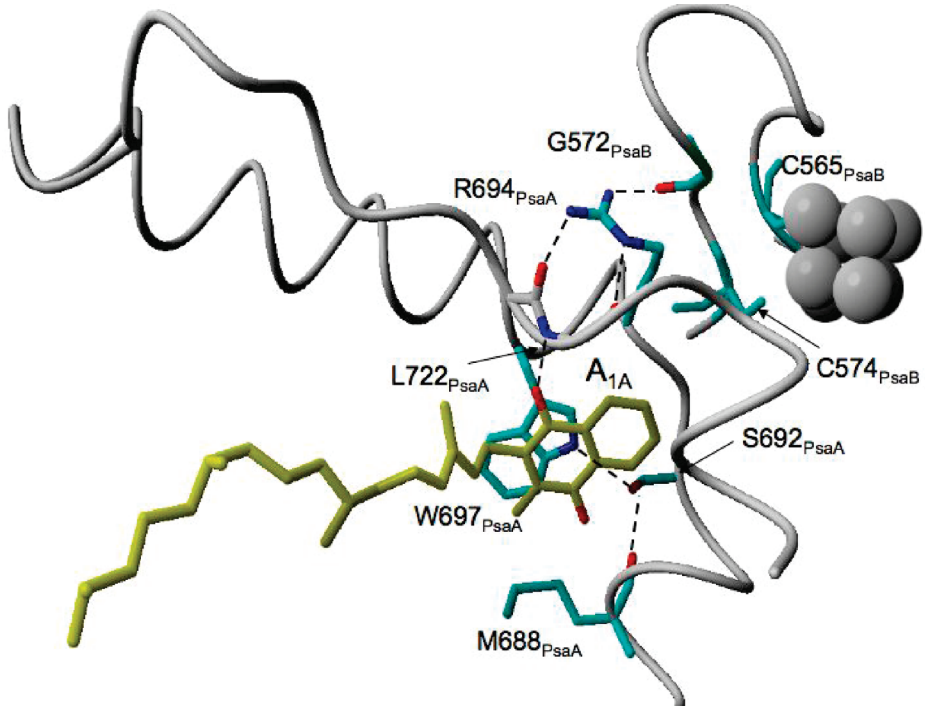

FIGURE 1: The phylloquinone binding pocket in PS I from the 2.5 Å X-ray crystal structure (*3*) (Protein Data Bank number 1JB0). The A_{1A} phylloquinone associated with the PsaA subunit is viewed parallel to the membrane plane.

proposed that electron transfer in the PsaB branch leads to stable charge separation between P_{700} and F_A/F_B whereas electron transfer through the PsaA branch leads to an electron cycle between P_{700} and A_{1A} (*7, 9*). One model that attempts to explain these observations suggests that electron transfer from A_{1A}^- to F_X is thermodynamically unfavorable while electron transfer from A_{1B}^- to F_X is thermodynamically favorable (*11*−*13*). This would be consistent with the observation that the slow phase of A_1^- oxidation exhibits a strong Arrhenius type temperature dependence with an activation energy of ∼110 meV, whereas the fast phase of A_1^- oxidation is nearly temperature independent, with an activation energy of ∼15 meV (*10, 11*). However, the factors that result in the two fractions are not fully understood at present.

For the fraction involved in reversible electron transfer, transient EPR, CW EPR, and pulsed ENDOR data on phylloquinone binding site mutants show no evidence for involvement of the PsaB-branch of cofactors (*7, 14*−*17*). However, when subjected to varying periods of illumination in the presence of a reductant to reduce the terminal iron−sulfur clusters, different spin polarized species are observed simultaneously and can be separated on the basis of their different kinetic behaviors. In out-of-phase electron spin echo experiments (*7, 9*) two different echo decay times of 2−4 μs and 16−25 μs are observed. The longer lifetime is attributed to the loss of spin correlation of the $P_{700}^{\bullet+}A_{1A}^{\bullet-}$ radical pair, while the component with the shorter lifetime is attributed to the $P_{700}^{\bullet+}A_{1B}^{\bullet-}$ radical pair. Under more stringent photoaccumulation conditions, A_{1A} can be completely reduced, in which case reversible electron transfer occurs between P_{700} and A_{1B} and between P_{700} and A_{0A} (*18, 19*). A spectrum attributed to the spin polarized $P_{700}^{\bullet+}A_{1B}^{\bullet-}$ radical pair has been obtained under these conditions using high-field (135 GHz) transient EPR spectroscopy and a kinetic analysis of the data. As predicted from the known geometry, the spin polarized EPR spectrum assigned to the $P_{700}^{\bullet+}A_{1B}^{\bullet-}$ radical pair is significantly different from that of the $P_{700}^{\bullet+}A_{1A}^{\bullet-}$ radical pair (*20*).

Figure 1 shows a view of the PsaA-branch phylloquinone binding pocket derived from the 2.5 Å X-ray crystal structure of cyanobacterial PS I. The two most striking features are (i) a Trp residue ($W697_{PsaA}/W677_{PsaB}$) in van der Waals contact with the phylloquinone, forming a π-stacked arrangement and (ii) a single hydrogen bond formed between the backbone amide of a Leu residue ($L722_{PsaA}/L706_{PsaB}$) and the oxygen atom of the C_4 carbonyl group meta to the methyl group of the phylloquinone. The presence of a single H-bond is most strongly supported by EPR and ENDOR studies on the photoaccumulated $A_1^{\bullet-}$ radical and on the spin correlated $P_{700}^{\bullet+}A_{1A}^{\bullet-}$ radical pair, both of which show an asymmetric spin density distribution on the phylloquinone ring (*21*−*24*). The presence of a H-bond is counterintuitive because its electron withdrawing ability would be expected to stabilize the semiquinone state relative to the ground state, which should lead to a higher (i.e., more oxidizing) midpoint potential (*25*). Given that the phylloquinones must function at highly reducing midpoint potentials, the surrounding protein environment must drive the redox potential lower (i.e., more reducing) than would otherwise be necessary to compensate for the effect of the H-bond. In light of these considerations, the relevant question becomes: what is the purpose of the H-bond?

Here, we focus on $L722_{PsaA}$, the residue involved in the formation of the single H-bond with the C_4 carbonyl group of the transient EPR-detectable A_{1A} phylloquinone. Because it is formed with the backbone nitrogen of $L722_{PsaA}$, the H-bond will not necessarily be affected by a simple change in the side chain of the amino acid. However, the introduction of a residue such as Trp, with a bulky side chain, might be expected to cause a reorientation of the A-jk(1) loop of the PsaA protein thereby weakening the H-bond to the phyllo-

quinone. In this paper, we describe the initial characterization of the L722W$_{PsaA}$ variant using low temperature transient EPR spectroscopy. The spin-polarized spectra of $P_{700}^{\bullet+}A_{1A}^{\bullet-}$ indicate that the spin density distribution on the phyllosemiquinone is altered in a manner that is consistent with a weakening of the hydrogen bond. The data suggest that the A_{1A} phylloquinone in the variant is highly susceptible to double reduction in the presence of dithionite in comparison to the wild-type. We propose that this difference arises because protonation of the phylloquinone, which is required for double reduction, occurs more easily when the H-bond is weakened. The selective alteration of the properties of the A_{1A} phylloquinone also allows the Q-band spectrum of the spin-polarized $P_{700}^{\bullet+}A_{1B}^{\bullet-}$ radical pair to be accurately recorded.

MATERIALS AND METHODS

Generation of the Point Mutants. The point mutant L722W$_{PsaA}$was generated as described in ref *15*. To generate mutations in the A_{1A} binding site, the pIBC plasmid was constructed through cloning of a DNA fragment that contained most of the *psaA* gene, the *psaB* gene and a 760-bp region downstream of the *psaB* gene into a pBluescript II KS vector. A chloramphenicol-resistant gene was inserted after the 3′ terminator of the *psaB* gene. PCR mutagenesis was carried out using the QuikChange site directed mutagenesis kit (Stratagene Inc.). The construct with the specific mutation in the *psaA* gene was generated through PCR mutagenesis using the pIBC plasmid DNA as the template and appropriate primers for L722W$_{PsaA}$. The plasmid with the desired *psaA* mutations derived from pIBC was used to transform the *Synechocystis* sp. PCC 6803 recipient strain pWX3. The pWX3 recipient strain was constructed by replacing the 1130-bp 3′ end of the *psaA* gene and the entire *psaB* gene with a spectinomycin resistance gene. Transformants with chloramphenicol resistance were selected under low light intensities. To verify the full segregation of the transformants, DNA fragments containing the mutation sites were amplified through PCR from the genomic DNA of the mutant strains and sequenced to confirm the desired nucleotide change.

Cell Culture and PS I Isolation. The *Synechocystis* sp. PCC 6803 wild-type and mutant strains were cultured in β-HEPES medium with 5 mM glucose under low light intensities. Preparation of thylakoid membranes and isolation of trimeric PS I particles were carried out using the nonionic detergent *n*-dodecyl-β-D-maltoside according to previously published procedures (*15*).

Multifrequency Spin-Polarized Transient EPR. The X-band (9 GHz) transient EPR experiments were carried out on a laboratory built spectrometer using a Bruker ER046 XK-T microwave bridge equipped with an ER-4118XMD-5W1 dielectric ring resonator and an Oxford CF935 helium gas flow cryostat. The loaded *Q*-value for this dielectric ring resonator was about 3000, equivalent to a risetime of $\tau_r = Q/(2\pi \times \nu_{mw}) \approx 50$ ns. Q-band (35 GHz) transient EPR spectra of the samples were also measured with the same setup except that a Bruker ER 056 QMV microwave bridge equipped with a home-built cylindrical resonator was used. All samples contained 1 mM sodium ascorbate as the external electron donor and were frozen in the dark. For the chemical reduction experiments, PS I complexes were incubated in the dark with 10 mM sodium dithionite at pH 10.0 under anaerobic conditions for 30 min and frozen in complete darkness. The samples were illuminated using a Spectra Physics Nd:YAG/MOPO laser system operating at 10 Hz.

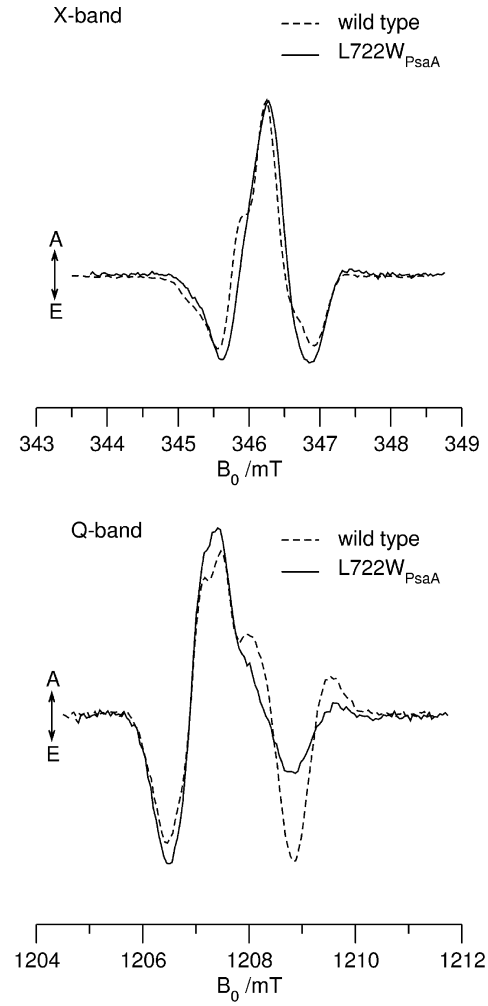

FIGURE 2: X-band (top) and Q-band (bottom) spin-polarized transient EPR spectra of PS I complexes isolated from L722W$_{PsaA}$ (solid lines) compared with wild-type (dashed lines) at 80 K. Positive signals correspond to absorption (A), and negative signals correspond to emission (E). The spectra represent the $P_{700}^{\bullet+}A_{1A}^{\bullet-}$ radical pair, and they have been extracted from full time/field data sets by averaging the signal intensity in a time window from 1.0 to 1.75 μs (X-band) and ~0.4 to 1.1 μs (Q-band) following the laser flash.

RESULTS

Low Temperature Spin-Polarized Transient EPR Spectra of $P_{700}^{\bullet+}A_{1A}^{\bullet-}$ at X- and Q-Bands. Figure 2 shows the low temperature spin-polarized transient EPR spectrum of PS I from the L722W$_{PsaA}$ variant at X-band and Q-band together with the corresponding wild-type spectrum. Note that the spectra are normalized to give the same maximum amplitude. The radical pair spectrum of the L722W$_{PsaA}$ variant shows an E/A/E (where E is emission and A is absorption; see ref *21* for a detailed discussion on the origin of the emissive and absorptive features in the spin-polarized transient EPR spectra of the $P_{700}^{\bullet+}A_1^{\bullet-}$ radical pair) polarization pattern at X-band and an E/A/A/E/A polarization pattern at Q-band that is similar to the wild-type but with some noticeable

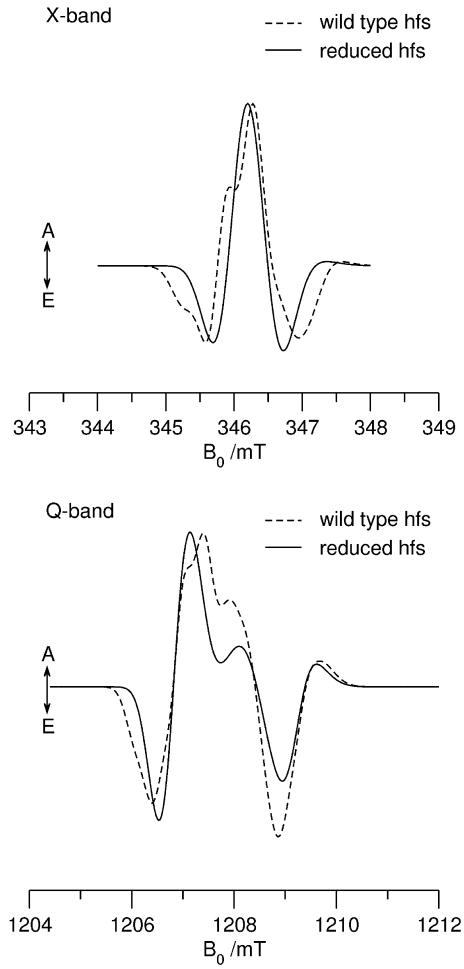

FIGURE 3: Simulated spectra of $P_{700}^{\bullet+}A_{1A}^{\bullet-}$ at X-band (top) and Q-band (bottom). The parameters are the same as those used in refs *26*, *27* except that in the solid spectra the principal values of the phylloquinone methyl hyperfine coupling have been reduced by a factor of 2.

differences. The most significant of these differences are the loss of the pronounced shoulder in the midfield region of the X-band spectrum and an increase in the amplitude of the low field E/A pattern relative to the high field emission in the Q-band spectrum. (With the chosen normalization, this appears as a decrease in the intensity in the upfield region.) The shoulder in the midfield region of the X-band spectrum is known to arise from the hyperfine coupling of the methyl group in the C_2 position on the phylloquinone headgroup. The loss of this shoulder in the $L722W_{PsaA}$ variant implies that the methyl hyperfine coupling has been weakened. Figure 3 shows numerical simulations in which the expected effect of a weakening of the methyl hyperfine coupling is explored. The dashed curves are calculations using the known parameters for the radical pair $P_{700}^{\bullet+}A_{1A}^{\bullet-}$ (*26, 27*). The solid curves are simulations using the same parameters except that the principal values of the methyl hyperfine coupling tensor have been reduced by a factor of 2. The spectra have been normalized to give the same maximum amplitude. The reduction of the methyl hyperfine coupling leads to the absence of the shoulder and an increase in the relative intensity of the low field region of the Q-band spectrum as observed experimentally. Thus, the spectra in Figure 2 indicate that the methyl hyperfine coupling is weaker in the $L722W_{PsaA}$ variant. The magnitude of the coupling is difficult

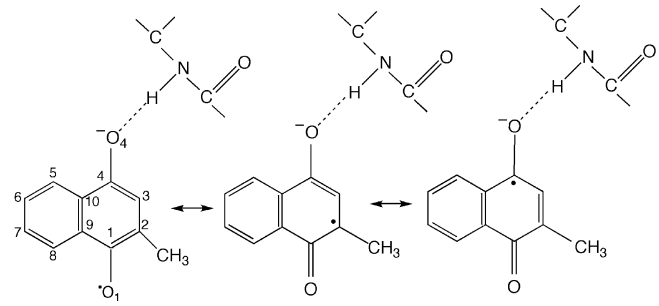

FIGURE 4: A valence bond scheme for the semiquinone π-radical anion involving a single H-bond. The electron withdrawing ability of the single H-bond increases the charge density on O_4 and the spin density on C_4 and creates an alternating electron spin density distribution in the ring. Three resonance structures are shown with the unpaired π-electron spin located at phylloquinone ring positions: 4, 2, and O_1 (right to left).

to estimate accurately from the spectra, thus the data only show qualitatively that the coupling has been reduced and is not a quantitative measure of the reduction. Nevertheless, the presence of methyl hyperfine couplings has proven to be a sensitive indicator of the environment of the phylloquinone from which the asymmetry and strength of the H-bond can be deduced (*23, 24*). In PS I from the wild-type, the H-bond withdraws electron density, producing an alternating pattern of electron spin density around the quinone ring as described by the valence bond model (Figure 4) such that the spin density is highest at C_2 and C_4, and lowest at C_1 and C_3. The interaction of the three methyl protons with the electron spin density on C_2 gives rise to a quartet with relative intensities 1:3:3:1 centered near the g_{yy} component of the electronic *g*-tensor of the quinone. In PS I from the $L722W_{PsaA}$ variant, the loss of the methyl hyperfine coupling indicates lower spin density on C_2, which can arise from a more symmetrical spin distribution due to either the absence of the single H-bond or the presence of two H-bonds of similar strength. The simplest explanation is that the bulky Trp has altered the configuration of the A-jk(1) loop containing residue $L722_{PsaA}$, thereby severely weakening the single H-bond to the phylloquinone.

In principle, the absence of the H-bond could lead to a lower binding constant for phylloquinone, resulting in a significant fraction of unfilled A_{1A} sites and/or an altered orientation of phylloquinone in the A_{1A} site. Both can be assessed by transient EPR spectroscopy. In the unfilled sites, the recombination between $P_{700}^{\bullet+}$ and $A_{0A}^{\bullet-}$ would generate a P_{700} triplet with a characteristic spin-polarized EPR spectrum. However, no such spectrum was detected in the $L722W_{PsaA}$ variant, implying that the A_{1A} sites are fully occupied (data not shown). The orientation of phylloquinone in the A_{1A} site is difficult to assess at X-band. However, at Q-band and higher frequencies, the spin polarization pattern of the $P_{700}^{\bullet+}A_{1A}^{\bullet-}$ radical pair is particularly sensitive to the relative orientation of the *g*-tensors $g(P_{700}^{\bullet+})$ and $g(A_{1A}^{\bullet-})$ with respect to the vector that connects the spin density centers involved in the radical pair (*21*). The fact that both the wild-type and the $L722W_{PsaA}$ variant have an E/A polarization pattern on the low-field side of their spectra (see Figure 2, bottom) indicates that the orientation of the A_{1A} phylloquinone in the variant is similar to the wild-type.

Low Temperature Spin-Polarized Transient EPR Spectra of Chemically Reduced PS I Complexes. Figure 5 shows the

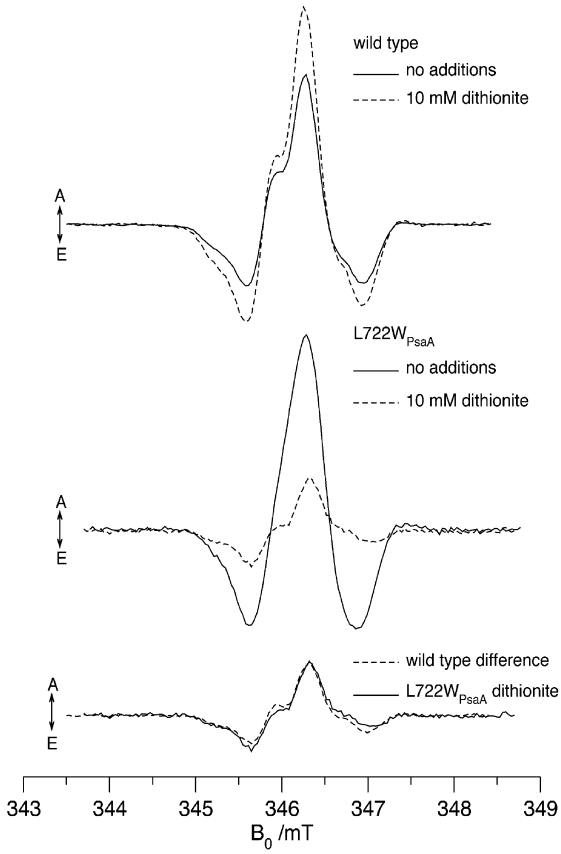

FIGURE 5: The effect of reduction by dithionite on the X-band spin-polarized transient EPR spectra of the wild-type (top) and L722W$_{PsaA}$ (middle). The top and middle parts of the figure show spectra measured at 80 K before (solid lines) and after (dashed lines) reduction. Note the opposite trend in the signal intensity between the wild-type and the mutant and the reappearance of the hfc structure upon reduction of L722W$_{PsaA}$. The bottom part of the figure shows a comparison of the spectrum of the L722W$_{PsaA}$ variant following reduction (solid lines) and the reduced minus nonreduced difference spectrum of the wild-type (dashed lines). The two spectra have been normalized to the same maximum absorption intensity. The E/A/E spectra of the nonreduced samples (solid traces top and middle) are attributed primarily to $P_{700}^{\bullet+}A_{1A}^{\bullet-}$ while the two spectra in the bottom trace are assigned to $P_{700}^{\bullet+}A_{1B}^{\bullet-}$. The contribution from $^3P_{700}$, which gives a sloping background to the spectra of the reduced wild-type and L722W$_{PsaA}$ samples, has been removed by a linear baseline correction.

low temperature X-band transient EPR spectrum of PS I from the wild-type and the L722W$_{PsaA}$ variant before and after chemical reduction of the terminal F_A/F_B clusters with sodium dithionite. In wild-type PS I, the most significant difference between the nonreduced and the reduced samples is the increase in signal intensity by 32%. This increase in the signal amplitude represents the irreversible fraction of PS I that would have passed electrons forward to the F_A/F_B clusters at low temperature, but are now forced to undergo reversible electron transfer between P_{700} and A_1. Contrary to expectation, a similar experiment resulted in an opposite trend in L722W$_{PsaA}$; here, the signal of the reduced sample decreased to 27% of the amplitude of the nonreduced sample.

The weaker $P_{700}^{\bullet+}A_1^{\bullet-}$ spectrum in the prereduced sample of the L722W$_{PsaA}$ variant suggests that the A_{1A} phylloquinone is more easily reduced to the phyllohydroquinone form than in the wild-type. It is also possible that the A_{1A} phyllohydroquinone is lost from the binding site in the L722W$_{PsaA}$ variant under reducing conditions since the phyllosemiquinone form is known to be somewhat labile in native PS I (*28, 29*). Consistent with double reduction and/or loss of the quinone, a strong spectrum of the triplet state of P_{700} is generated due to the recombination of $P_{700}^{\bullet+}$ and $A_0^{\bullet-}$ (data not shown). Closer inspection of Figure 5 (middle) shows that the shape of the $P_{700}^{\bullet+}A_1^{\bullet-}$ spectrum from the L722W$_{PsaA}$ variant also changes when the sample is reduced. The most noticeable differences are the reappearance of the shoulder on the central absorptive peak of the reduced L722W$_{PsaA}$ sample, indicative of partially resolved methyl hyperfine splitting, and a change in the relative intensity of the emissive feature on the high field end of the spectrum. Since the simplest explanation for the EPR spectrum of the untreated samples in Figures 2 and 5 is that the H-bond between the protein and the A_{1A} phylloquinone is disrupted in the L722W$_{PsaA}$ variant, the reappearance of the hyperfine coupling upon dithionite treatment must be either due to a small population of A_{1A} that has re-established the H-bond or due to electron transfer involving the A_{1B} phylloquinone in which the H-bond from L706$_{PsaB}$ remains unaltered.

Figure 6 compares the X- and Q-band spectra of the reduced L722W$_{PsaA}$ variant with a nonreduced wild-type sample. The spectra have been normalized to the same intensity in the low-field region, which is dominated by the contribution from the phylloquinone to the spin polarized radical pair. As can be seen in the Q-band spectrum, the $P_{700}^{\bullet+}A_1^{\bullet-}$ polarization pattern changes from E/A/A/E/A in the wild-type to E/A/E/A/E in the chemically reduced L722W$_{PsaA}$ variant, with the maximum change occurring in the high field region of the spectrum. The fact that the two spectra are different clearly suggests that the spectrum of the variant is not due to a fraction of the complexes in which the H-bond to A_{1A} is re-established. Instead, the spectrum of the reduced variant appears to represent the spin-polarized EPR spectrum of the $P_{700}^{\bullet+}A_{1B}^{\bullet-}$ radical pair that becomes observable after (i) blocking forward electron transfer from $A_{1B}^{\bullet-}$ via F_X to F_A and F_B, and (ii) blocking electron transfer from $A_{0A}^{\bullet-}$ to A_{1A}.

A similar hypothesis is invoked to explain the observations on the reduced wild-type sample, in which the formation of a trapped fraction via electron transfer through the PsaB-branch leads to the increase in signal intensity (*7, 9*). If correct, the increase in the intensity of the wild-type $P_{700}^{\bullet+}A_1^{\bullet-}$ spectrum upon reduction of F_A and F_B would be due to an additional contribution from the PsaB-branch radical pair $P_{700}^{\bullet+}A_{1B}^{\bullet-}$. Hence the difference between the spectra of the reduced and nonreduced wild-type samples should produce the spectrum of the PsaB-branch radical pair. The bottom trace in Figure 5 shows a comparison of this difference spectrum and the spectrum of the reduced L722W$_{PsaA}$ variant. As can be seen, their shapes are indeed the same, which strongly suggests they are both due to $P_{700}^{\bullet+}A_{1B}^{\bullet-}$.

Simulation of the Low Temperature X- and Q-Band Spin-Polarized Transient EPR Spectra. The spectra of $P_{700}^{\bullet+}A_{1A}^{\bullet-}$ and $P_{700}^{\bullet+}A_{1B}^{\bullet-}$ differ because the spin density on $P_{700}^{\bullet+}$ is localized on the Chl *a* molecule associated with PsaB (*30, 31*) which leads to a different orientation of the dipolar coupling vector relative to the *g*-tensor axes of $P_{700}^{\bullet+}$ in the radical pairs $P_{700}^{\bullet+}A_{1A}^{\bullet-}$ and $P_{700}^{\bullet+}A_{1B}^{\bullet-}$. To confirm that the spin-polarized spectrum of the reduced L722W$_{PsaA}$ sample represents the $P_{700}^{\bullet+}A_{1B}^{\bullet-}$ radical pair, numerical simulations

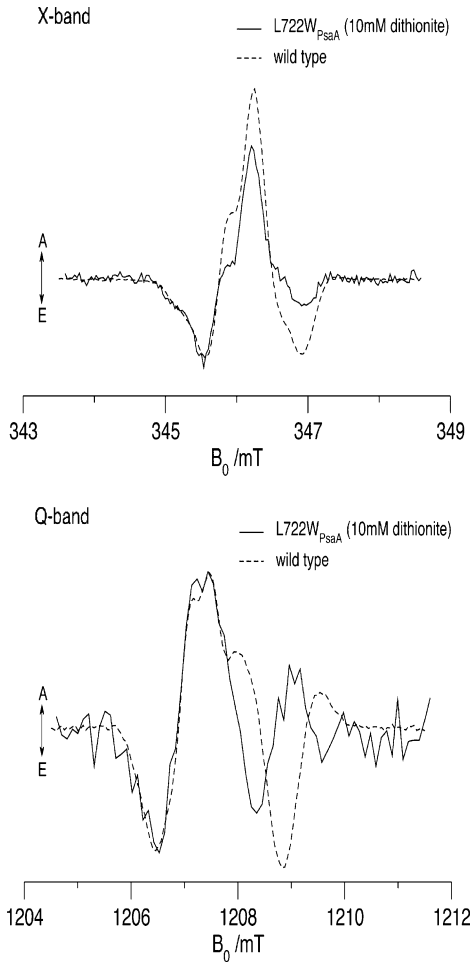

FIGURE 6: X-band (top) and Q-band (bottom) spin-polarized transient EPR spectra of wild-type (dashed lines) and reduced L722W$_{PsaA}$ (solid lines) recorded at 80 K. The difference is more prominent at Q-band. The E/A/A/E/A polarization pattern in the wild-type changes to E/A/E/A/E in reduced L722W$_{PsaA}$. The contribution from $^3P_{700}$, which gives a sloping background to the spectra of the reduced L722W$_{PsaA}$ sample, has been removed by a linear baseline correction. The spectra are normalized to give the same amplitude for the low-field emissive feature.

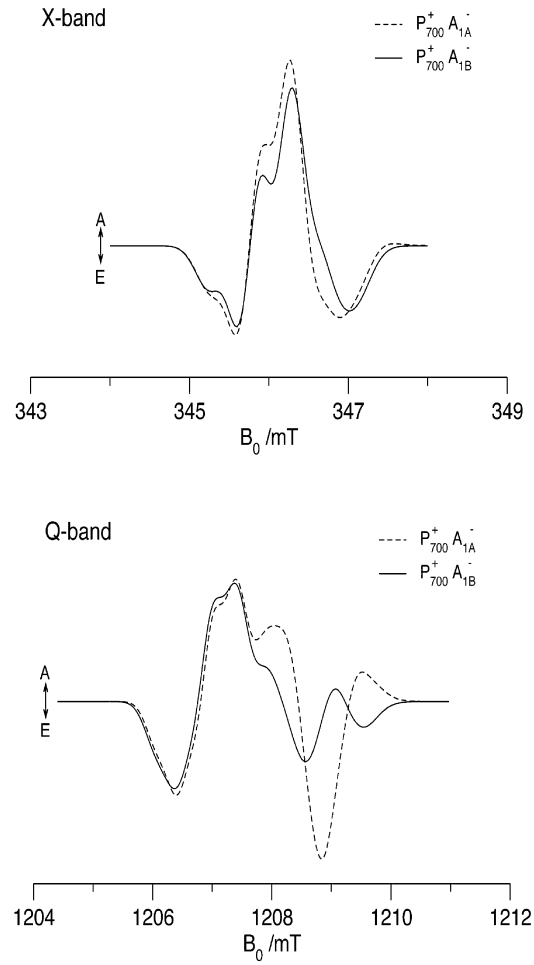

FIGURE 7: Simulated X-band (top) and Q-band (bottom) spin-polarized transient EPR spectra of $P_{700}^{\bullet+}A_{1A}^{\bullet-}$ (dashed lines) and $P_{700}^{\bullet+}A_{1B}^{\bullet-}$ (solid lines). Euler angles in degrees as defined in ref *32* describing $g(A_1)$ in $g(P_{700}^+)$: $P_{700}^{\bullet+}A_{1A}^{\bullet-}$ (26, 126, 81); $P_{700}^{\bullet+}A_{1B}^{\bullet-}$ (101, 80, −220). Angles θ and ϕ describing the dipolar vector z_d in $g(P_{700}^+)$ in degrees: $P_{700}^{\bullet+}A_{1A}^{\bullet-}$ (36, 78); $P_{700}^{\bullet+}A_{1B}^{\bullet-}$ (87, 75). All other parameters are the same as those used in refs *26*, *27*.

were carried out (Figure 7) using geometric parameters calculated from the X-ray structural model and known orientation of the *g*-tensor axes of $P_{700}^{\bullet+}$ and the phyllosemiquinones in their respective molecular frames (*26*). The angles describing the relative orientations of the dipolar coupling vector and the two *g*-tensors are given in the caption to Figure 7 (*32*). All other parameters used in the simulation are the same as given in refs *26* and *27*. As can be seen from the comparison of Figure 6 and Figure 7, the numerical simulations of $P_{700}^{\bullet+}A_{1A}^{\bullet-}$ and $P_{700}^{\bullet+}A_{1B}^{\bullet-}$ closely resemble the spectra of the wild-type and the L722W$_{PsaA}$ variant following reduction by dithionite respectively, which supports the idea that the spectrum of the reduced L722W$_{PsaA}$ variant is due to electron transfer through the PsaB-side cofactors.

DISCUSSION

Effect of the Mutation on the Strength of the H-Bond. The relative strength of the H-bond from the backbone nitrogen of Leu722$_{PsaA}$ to the A_{1A} phylloquinone can be assessed using transient EPR spectroscopy. The distinct absence of the methyl hyperfine coupling observed in the L722W$_{PsaA}$ variant can come about as a result of a more symmetrical spin density distribution, either from a second H-bond, in this instance to the C_1 carbonyl group of the phylloquinone, or a weakened H-bond, in this instance from L722$_{PsaA}$ to the C_4 carbonyl group. Under both conditions, the electron spin density distribution at C_2 would be decreased, leading to a weaker hyperfine coupling with the methyl protons. This is because the H-bond to the phylloquinone in the A_{1A} site has a large effect on the spin density distribution around the quinone ring. The highest spin and charge density in a phylloquinone radical anion is expected at the two carbonyl groups because of the high electronegativity of the oxygen atoms. Formally, the charge is placed on the oxygen, while the unpaired electron is placed on the carbon. In vacuum or a homogeneous protic solvent, in which H-bonding to the two oxygen atoms is the same, the spin density on C_1 and C_4 is identical. In contrast, when a single H-bond is present at O_4, its electron withdrawing effect is expected to increase the charge on O_4 and the spin density at C_4 compared to O_1 and C_1, respectively. In accordance with the resonance structures of a conjugated system, the single H-bond leads to an alternating electron spin density distribution in the ring such that it is highest at C_4 and C_2 and lowest at C_3 and C_1

(Figure 4). It is the high spin density at C_2 that is responsible for the pronounced hyperfine coupling from the $-CH_3$ group of phylloquinone in wild-type PS I. Turning the argument around, the magnitude of the methyl hyperfine coupling can serve as a sensitive probe of the strength and number of H-bonds to the A_{1A} phylloquinone.

The crystal structure of PS I at 2.5 Å resolution shows that the side chain of $L722_{PsaA}$ points away from the A_{1A} site, suggesting that, upon substitution of a Trp residue, the bulky imidazole side chain would not result in steric hindrance and therefore not interfere with side chains that make up the phylloquinone binding pocket. Consistent with this expectation, the transient EPR data do not show any significant alteration in the orientation of the semiquinone ring with respect to $P_{700}^{\bullet+}$, indicating that the change in the H-bond strength is probably a result of alterations of the conformation of the protein backbone near $L722_{PsaA}$. One possibility is that the A-jk(1) switchback loop, which contains the $L722_{PsaA}$ residue, moves from its normal equilibrium position, thereby weakening the single H-bond to the A_{1A} quinone. A second possibility is that more distant shifts in the protein backbone would allow for the formation of a second H-bond with the C_1 carbonyl group. These two possibilities can be distinguished because the rate of electron transfer from A_{1A}^- to F_X in the $L722W_{PsaA}$ variant is sensitive to the number and strength of the H-bonds. A weaker H-bond would be expected to shift the midpoint potential of A_{1A} to a more negative value, and thereby increase the driving force for electron transfer from A_{1A}^- to F_X. A second H-bond would be expected to shift the midpoint potential of A_{1A} to a more positive value, and thereby decrease the driving force for electron transfer from A_{1A}^- to F_X. Preliminary measurements carried out at 240 K show that the rate of electron transfer from A_{1A}^- to F_X increases by about an order of magnitude compared to the wild-type, thereby favoring the simpler hypothesis that a single H-bond is weakened rather than the more complicated hypothesis that a second H-bond is formed (*33*). We are currently exploring possible configurations for the PS I variant using molecular mechanics simulations to determine the new equilibrium position of the A-jk(1) loop. The temperature study of forward electron transfer as well as the molecular mechanics simulations will be discussed elsewhere.

Reversible and Irreversible Electron Transfer to the A_{1A} and A_{1B} Phylloquinones. Chemical reduction with sodium dithionite leads to very different effects in PS I from the wild-type and the $L722W_{PsaA}$ variant. At temperatures below 100 K, ~75% of wild-type PS I undergoes reversible electron transport between P_{700} and the A_{1A} phylloquinone, generating the transient EPR-observable $P_{700}^{\bullet+}A_{1A}^{\bullet-}$ radical pair (*10*). The other ~25% of the reaction centers do not contribute to the transient EPR spectrum because, on the first several flashes, irreversible $P_{700}^+ [F_A/F_B]^-$ charge separated pair is formed. In the currently proposed model, irreversible electron transfer to F_A and F_B proceeds via the A_{1B} phylloquinone. When F_A and F_B are chemically reduced, this otherwise transient EPR silent fraction begins to undergo reversible electron transfer and its contribution adds to the amplitude of the $P_{700}^{\bullet+}$ $A_{1A}^{\bullet-}$ radical pair spectrum, increasing its intensity by ~25%. The results presented here also suggest that this contribution arises from PsaB-side electron transfer.

The chemically reduced $L722W_{PsaA}$ sample behaves differently. Three significant features require further elaboration: (i) the decrease in the amplitude of the radical pair spectrum after reduction of F_A and F_B; (ii) the reappearance of the prominent methyl hyperfine couplings; and (iii) the formation of spin-polarized P_{700} triplet. If the H-bond were weakened, as we suspect is the case in the $L722W_{PsaA}$ variant, the A_{1A} phylloquinone might become susceptible to protonation and undergo facile double reduction. The alteration in the equilibrium position of the A-jk(1) switchback loop could further result in the opening of a water channel, allowing for easier protonation. Were this to occur, forward electron transfer to F_X (as well as backward electron transfer to A_0) would be blocked because the phyllosemiquinone/phylloquinone couple has a higher (more positive) redox potential than the phylloquinone/phyllosemiquinone couple (*18*). The 3/4 fraction of PS I complexes that had originally given rise to the $P_{700}^{\bullet+}A_{1A}^{\bullet-}$ radical pair would now become transient EPR silent, leading to a decrease in the spectral amplitude. We propose that the spin-polarized signal in the chemically reduced $L722W_{PsaA}$ variant represents the population of PS I that was transient EPR silent in the nonreduced sample. This fraction would correspond to the population of PS I that irreversibly charge separates at low temperature to $P_{700}^+ [F_A/F_B]^-$. The reappearance of the methyl hyperfine coupling in the X-band spectrum shows the involvement of a quinone with an intact H-bond, supporting the proposal that the spectra arise from the spin-polarized $P_{700}^{\bullet+}A_{1B}^{\bullet-}$ radical pair. The observation that upon chemical reduction the spin polarization pattern of the $L722W_{PsaA}$ variant becomes equivalent to that of the difference spectrum (reduced minus nonreduced) of the wild-type provides excellent support to the above argument. In the fraction of PS I complexes in which electron transport past A_0 is blocked, charge recombination would occur between P_{700}^+ and A_0^-. During such recombination two products are formed: the singlet P_{700} species (yield ~70%) and the triplet P_{700} species (yield ~30%) that decay by intersystem crossing to the singlet ground state in a few microseconds (see ref *34*). Consistent with this picture, a strong triplet P_{700} is observed in the reduced $L722W_{PsaA}$ variant. However, quantification of the amplitude and comparison with the wild type are complicated by the possibility of stable reduction of A_0 in the variant and A_1 in the wild type. Hence, the intensity of the triplet spectrum is difficult to use as a quantitative measure of the amount of electron transfer beyond A_0. Nonetheless, it is reasonable to conclude that the observed P_{700} triplet signal together with the 75% decrease in the radical pair signal strength indicates an essentially complete block in PsaA-side electron transfer past A_0 in the $L722W_{PsaA}$ variant under reducing conditions.

Spectrum of the Spin-Polarized $P_{700}^{\bullet+}A_{1B}^{\bullet-}$ Radical Pair. The differences in the spectra of the two radical pairs $P_{700}^{\bullet+}A_{1A}^{\bullet-}$ and $P_{700}^{\bullet+}A_{1B}^{\bullet-}$ arise from the difference in the spin density distribution on $P_{700}^{\bullet+}$. The 2.5 Å resolution X-ray crystal structure of PS I shows that the two branches of cofactors are arranged symmetrically about an axis that passes through P_{700} and F_X (*3*). This structural symmetry does not, however, translate to electronic symmetry (Figure 8). The spin density distribution on $P_{700}^{\bullet+}$ is asymmetric with the spin mainly localized on the Chl *a* molecule ligated by the PsaB subunit (*30, 31*). As a result of this asymmetry the

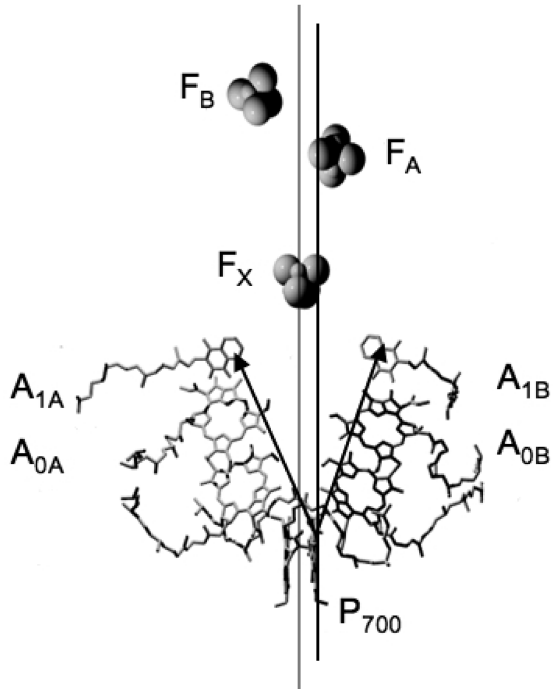

FIGURE 8: The arrangement of cofactors in PS I from the 2.5 Å X-ray crystal structure seen parallel to the membrane plane (*3*). A vertical axis in gray passes through F_X representing the C_2 axis of symmetry. The axis in black passes through the Chl *a* molecule of P_{700} ligated by PsaB, on which the majority of the charge on $P_{700}^{\bullet+}$ is localized. The vector connecting the centers of $P_{700}^{\bullet+}$ and $A_1^{\bullet-}$ is oriented differently relative to the *g*-tensor axis of $P_{700}^{\bullet+}$ in the two radical pairs, $P_{700}^{\bullet+}A_{1A}^{\bullet-}$ and $P_{700}^{\bullet+}A_{1B}^{\bullet-}$.

vector z_d, which connects the centers of $P_{700}^{\bullet+}$ and $A_1^{\bullet-}$, is oriented differently relative to the *g*-tensor axes of P_{700}^{+} in the two radical pairs. This difference has a considerable effect on the $P_{700}^{\bullet+}$ region of the spin polarization pattern of the transient EPR spectrum as can be seen in the simulated spectra shown in Figure 7 and in ref *20*. Consistent with this effect, the transient EPR spectra of the photoaccumulated sample (*20*) and the $L722W_{PsaA}$ mutant (this work) show the largest change in the high-field region of the spectrum, where the main contribution is derived from $P_{700}^{\bullet+}$. Based on the similarity between the observed Q-band spectrum and the simulated $P_{700}^{\bullet+}A_{1B}^{\bullet-}$ spectrum, the presence of resolved hyperfine coupling in the X-band spectrum and the large decrease in intensity upon reduction, we conclude that the spectrum of the reduced $L722W_{PsaA}$ sample arises primarily from $P_{700}^{\bullet+}A_{1B}^{\bullet-}$. In an alternate scenario, a shift of the asymmetric spin distribution of $P_{700}^{\bullet+}$ from the B-branch Chl *a* to the A-branch Chl *a*′ such that the interspin vector connects the Chl *a*' and $A_{1A}^{\bullet-}$ could result in an identical spectrum. This possibility is less likely for two reasons: (i) such redistribution would require a perturbation around P_{700}, which is not expected at a distance so far from $L722_{PsaA}$, and (ii) the appearance of the hyperfine coupling in the X-band spectrum of the reduced $L722W_{PsaA}$ sample indicates the involvement of the unmodified A_{1B} site rather than the modified A_{1A} site. The involvement of A_{1B} is further supported by the similarity between the difference spectrum of the reduced and nonreduced wild-type and the reduced $L722W_{PsaA}$ variant shown in Figure 5. Thus, the results for the $L722W_{PsaA}$ variant are in agreement with the findings of Poluektov et al. (*20*), who showed that when A_{1A} is completely reduced, a spin-polarized spectrum consistent with the $P_{700}^{\bullet+}A_{1B}^{\bullet-}$ radical pair is obtained.

Phylloquinone−protein Interactions Necessary for Binding to the A_{1A} Site. To understand the influence of the protein environment on the functional properties of any given cofactor, it is necessary to restrict changes to the near vicinity of the cofactor. This is especially true in the case of phylloquinone, as the route of electron transfer along the PsaA- and PsaB-branches is likely to be completely decided prior to the A_{0A} to A_{1A} (and A_{0B} to A_{1B}) electron transfer steps. Phylloquinone is tightly bound in the A_{1A} and A_{1B} binding sites, but the interactions that anchor it to the protein appear to be primarily hydrophobic (i.e., entropic). Nevertheless, a wide range of structurally different compounds are able to bind to the A_{1A} and A_{1B} sites. If the 2-methyl group is removed, the 2-phytyl-1,4-naphthoquinone tightly occupies the A_{1A} site in an orientation similar to phylloquinone in the wild-type (*35*) (see ref *36* for a review of quinone substitution studies). The only effect is a predictable slowing of electron transfer due to a positive shift in the midpoint potential of the quinone. If the phytyl tail of phylloquinone is removed, the 2-methyl-1,4-naphthoquinone occupies the A_{1A} site also in an orientation similar to phylloquinone in the wild-type (*24, 37*) and again the forward electron transfer kinetics from A_{1A} are altered in agreement with a positive shift in the midpoint potential of the 2-methyl-1,4-naphthoquinone. Plastoquinone-9, which is a single ring quinone with a much longer tail, can be recruited into the A_{1A} site and is also oriented similar to that of phylloquinone in the wild-type (*38*−*42*). However, in contrast to the modified phylloquinones, it is loosely bound and can be easily displaced by a variety of substituted 1,4-naphthoquinones. Studies using solvent extracted PS I have shown that anthraquinones also bind while benzoquinones often bind poorly (*43*−*46*). In all of the studies involving naphthoquinone derivatives, the EPR parameters indicate that the H-bond from $L722_{PsaA}$ to the C_4 carbonyl group of the phylloquinone in the A_{1A} site (and from $L706_{PsaB}$ to the C_4 carbonyl group of an equivalent phylloquinone in the A_{1B} site) is retained. However, as shown in this work, the H-bond is structurally dispensable: phylloquinone occupies the A_{1A} site with an orientation similar to that in the wild-type. Thus, any one of the three most prominent features of phylloquinone—the C_2 methyl group, the C_3 phytyl tail, or the C_4 H-bond—can be altered (or eliminated) and yet the phylloquinone binds in the A_{1A} site and functions in electron transfer. Given that the presence of the H-bond requires the protein environment to drive the redox potential more reducing than would otherwise be necessary and given that the H-bond does not serve a structural role in binding or orienting phylloquinone in the A_{1A} and by inference in the A_{1B} site, its role must be sought elsewhere. We propose that because the A_{1A} phylloquinone in the $L722W_{PsaA}$ variant is inactivated under reducing conditions, the primary role of the H-bond between the A_{1A} phylloquinone and the protein backbone is to ensure function of the phylloquinone between its oxidized and singly reduced states. The presence of the H-bond would tie up the C_4 carbonyl group, preventing protonation and rendering the phylloquinone less susceptible to double reduction and possible dissociation from the binding site under periods of high illumination. The phylloquinone in cyanobacterial PS I complexes has been shown

to undergo double reduction when illuminated in the presence of sodium dithionite (*18, 19*). The transient accumulation of reduced electron acceptors, F_B^-, F_A^-, F_X^-, and A_1^-, upon illuminating dark-adapted cyanobacterial cells (*41, 47*) indicates that double reduction of phylloquinone may be a realistic occurrence under physiologically relevant conditions.

ACKNOWLEDGMENT

We thank Dr. Gaozhong Shen for helpful advice in the construction of the mutant.

REFERENCES

1. Schubert, W. D., Klukas, O., Saenger, W., Witt, H. T., Fromme, P., and Krauss, N. (1998) A common ancestor for oxygenic and anoxygenic photosynthetic systems: A comparison based on the structural model of photosystem I. *J. Mol. Biol. 280*, 297–314.
2. Chitnis, P. R., Xu, Q., Chitnis, V. P., and Nechushtai, R. (1995) Function and organization of Photosystem I polypeptides. *Photosynth. Res. 44*, 23–40.
3. Jordan, P., Fromme, P., Witt, H. T., Klukas, O., Saenger, W., and Krauβ, N. (2001) Three dimensional structure of Photosystem I at 2.5 Å resolution. *Nature 411*, 909–917.
4. Guergova-Kuras, M., Boudreaux, B., Joliot, A., Joliot, P., and Redding, K. (2001) Evidence for two active branches for electron transfer in Photosystem I. *Proc. Natl. Acad. Sci. U.S.A. 98*, 4437–4442.
5. Joliot, P., and Joliot, A. (1999) In vivo analysis of the electron transfer within Photosystem I: are the two phylloquinones involved? *Biochemistry 38*, 11130–11136.
6. Bautista, J. A., Rappaport, F., Guergova-Kuras, M., Cohen, R. O., Golbeck, J. H., Wang, J. Y., Beal, D., and Diner, B. A. (2005) Biochemical and biophysical characterization of Photosystem I from phytoene desaturase and zeta-carotene desaturase deletion mutants of *Synechocystis* sp. PCC 6803: Evidence for PsaA- and PsaB-side electron transport in cyanobacteria. *J. Biol. Chem. 280*, 20030–20041.
7. Muhiuddin, I. P., Heathcote, P., Carter, S., Purton, S., Rigby, S. E., and Evans, M. C. (2001) Evidence from time resolved studies of the $P_{700}^{\bullet+}A_1^{\bullet-}$ radical pair for photosynthetic electron transfer on both the PsaA and PsaB branches of the Photosystem I reaction centre. *FEBS Lett. 503*, 56–60.
8. Santabarbara, S., Kuprov, I., Fairclough, W. V., Purton, S., Hore, P. J., Heathcote, P., and Evans, M. C. (2005) Bidirectional electron transfer in Photosystem I: determination of two distances between P_{700}^+ and A_1^- in spin-correlated radical pairs. *Biochemistry 44*, 2119–2128.
9. Santabarbara, S., Kuprov, I., Hore, P. J., Casal, A., Heathcote, P., and Evans, M. C. (2006) Analysis of the spin-polarized electron spin echo of the P_{700}^+ A_1^- radical pair of Photosystem I indicates that both reaction center subunits are competent in electron transfer in cyanobacteria, green algae, and higher plants. *Biochemistry 45*, 7389–7403.
10. Schlodder, E., Falkenberg, K., Gergeleit, M., and Brettel, K. (1998) Temperature dependence of forward and reverse electron transfer from A_1^-, the reduced secondary electron acceptor in Photosystem I. *Biochemistry 37*, 9466–9476.
11. Agalarov, R., and Brettel, K. (2003) Temperature dependence of biphasic forward electron transfer from the phylloquinone(s) A_1 in Photosystem I: only the slower phase is activated. *Biochim. Biophys. Acta 1604*, 7–12.
12. Santabarbara, S., Heathcote, P., and Evans, M. C. (2005) Modelling of the electron transfer reactions in Photosystem I by electron tunnelling theory: the phylloquinones bound to the PsaA and the PsaB reaction centre subunits of PS I are almost isoenergetic to the iron-sulfur cluster F_X. *Biochim. Biophys. Acta 1708*, 283–310.
13. Ishikita, H., and Knapp, E. W. (2003) Redox potential of quinones in both electron transfer branches of Photosystem I. *J. Biol. Chem. 278*, 52002–52011.
14. Boudreaux, B., MacMillan, F., Teutloff, C., Agalarov, R., Gu, F., Grimaldi, S., Bittl, R., Brettel, K., and Redding, K. (2001) Mutations in both sides of the Photosystem I reaction center identify the phylloquinone observed by electron paramagnetic resonance spectroscopy. *J. Biol. Chem. 276*, 37299–37306.
15. Xu, W., Chitnis, P., Valieva, A., van der Est, A., Pushkar, Y. N., Krzystyniak, M., Teutloff, C., Zech, S. G., Bittl, R., Stehlik, D., Zybailov, B., Shen, G., and Golbeck, J. H. (2003) Electron transfer in cyanobacterial Photosystem I: I. Physiological and spectroscopic characterization of site-directed mutants in a putative electron transfer pathway from A_0 through A_1 to F_X. *J. Biol. Chem. 278*, 27864–27875.
16. Xu, W., Chitnis, P. R., Valieva, A., van der Est, A., Brettel, K., Guergova-Kuras, M., Pushkar, Y. N., Zech, S. G., Stehlik, D., Shen, G., Zybailov, B., and Golbeck, J. H. (2003) Electron transfer in cyanobacterial Photosystem I: II. Determination of forward electron transfer rates of site-directed mutants in a putative electron transfer pathway from A_0 through A_1 to F_X. *J. Biol. Chem. 278*, 27876–27887.
17. Purton, S., Stevens, D. R., Muhiuddin, I. P., Evans, M. C., Carter, S., Rigby, S. E., and Heathcote, P. (2001) Site-directed mutagenesis of PsaA residue W693 affects phylloquinone binding and function in the Photosystem I reaction center of *Chlamydomonas reinhardtii*. *Biochemistry 40*, 2167–2175.
18. Bottin, H., and Setif, P. (1991) Inhibition of electron transfer from A_0 to A_1 in Photosystem I after treatment in darkness at low redox potential. *Biochim. Biophys. Acta 1057*, 331–336.
19. Heathcote, P., Hanley, J. A., and Evans, M. C. W. (1993) Double-reduction of A_1 abolishes the EPR signal attributed to A_1^-. Evidence for C_2 symmetry in the Photosystem I reaction center. *Biochim. Biophys. Acta 1144*, 54–61.
20. Poluektov, O. G., Paschenko, S. V., Utschig, L. M., Lakshmi, K. V., and Thurnauer, M. C. (2005) Bidirectional electron transfer in Photosystem I: direct evidence from high-frequency time-resolved EPR spectroscopy. *J. Am. Chem. Soc. 127*, 11910–11911.
21. Stehlik, D. (2006) Transient EPR spectroscopy as applied to light-induced functional intermediates along the electron transfer pathway in Photosystem I, in *Photosystem I: The Light-Driven Plastocyanin: Ferredoxin Oxidoreductase* (Golbeck, J., Ed.) pp 361−386, Springer, Dordrecht.
22. Rigby, S. E., Evans, M. C., and Heathcote, P. (2001) Electron nuclear double resonance (ENDOR) spectroscopy of radicals in Photosystem I and related Type 1 photosynthetic reaction centres. *Biochim. Biophys. Acta 1507*, 247–259.
23. Karyagina, I., Golbeck, J. H., Srinivasan, N., Stehlik, D., and Zimmermann, H. (2006) Single-sided hydrogen bonding to the quinone cofactor in Photosystem I probed by selective ^{13}C labelled naphthoquinones and transient EPR. *Appl. Magn. Reson. 30*, 287–310.
24. Pushkar, Y. N., Golbeck, J. H., Stehlik, D., and Zimmermann, H. (2004) Asymmetric hydrogen-bonding of the quinone cofactor in Photosystem I probed by ^{13}C labeled naphthoquinones. *J. Phys. Chem. B 108*, 9439–9448.
25. Feldman, K. S., Hester, D. K., 2nd, and Golbeck, J. H. (2007) A relationship between amide hydrogen bond strength and quinone reduction potential: Implications for Photosystem I and bacterial reaction center quinone function. *Bioorg. Med. Chem. Lett. 17*, 4891–4894.
26. Zech, S. G., Hofbauer, W., Kamlowski, A., Fromme, P., Stehlik, D., Lubitz, W., and Bittl, R. (2000) A structural model for the charge separated state P_{700}^+ A_1^- in Photosystem I from the orientation of the magnetic interaction tensors. *J. Phys. Chem. B 104*, 9728–9739.
27. Kandrashkin, Y. E., Vollmann, W., Stehlik, D., Salikhov, K., and van der Est, A. (2002) The magnetic field dependence of the electron spin polarization in consecutive spin correlated radical pairs in type I photosynthetic reaction centres. *Mol. Phys. 100*, 1431–1443.
28. Ostafin, A. E., and Weber, S. (1997) Quinone exchange at the A_1 site in Photosystem I in spinach and cyanobacteria. *Biochim. Biophys. Acta 1320*, 195–207.
29. Rustandi, R. R., Snyder, S. W., Biggins, J., Norris, J. R., and Thurnauer, M. C. (1992) Reconstitution and exchange of quinones in the A_1 site of Phototsystem I. An electron spin polarization electron paramagnetic resonance study. *Biochim. Biophys. Acta 1011*, 311–320.
30. Kass, H., Fromme, P., Witt, H. T., and Lubitz, W. (2001) Orientation and electronic structure of the primary donor radical cation P_{700}^+ in Photosystem I: A single crystals EPR and ENDOR study. *J. Phys. Chem. B 105*, 1225–1239.
31. Webber, A. N., and Lubitz, W. (2001) P_{700}: the primary electron donor of Photosystem I. *Biochim. Biophys. Acta 1507*, 61–79.
32. van der Est, A., Prisner, T., Bittl, R., Fromme, P., Lubitz, W., Mobius, K., and Stehlik, D. (1997) Time-resolved X-, K- and W-band EPR of the radical pair state $P_{700}^+A_1^-$ of Photosystem I

in comparison with $P_{865}^{+}Q_A^{-}$ in bacterial reaction centers. *J. Phys. Chem. B 101*, 1437–1443.

33. Shrinivasan, N., Karyagina, I., Golbeck, J. H., and Stehlik, D. (2007) Structure function correlations in the ($A_0 \rightarrow A_1 \rightarrow F_X$) electron transfer kinetics of the phylloquinone (A_1) acceptor in cyanobacterial Photosystem I, in *Photosynthesis. Energy from the sun: 14th International Congress on Photosynthesis* (Allen, J. F., Gantt, E., Golbeck, J. H., and Osmond, B., Eds.) pp 207−210, Springer, Dordrecht.
34. Polm, M., and Brettel, K. (1998) Secondary pair charge recombination in Photosystem I under strongly reducing conditions: Temperature dependence and suggested mechanism. *Biophys. J. 74*, 3173–3181.
35. Sakuragi, Y., Zybailov, B., Shen, G., Jones, A. D., Chitnis, P. R., van der Est, A., Bittl, R., Zech, S., Stehlik, D., Golbeck, J. H., and Bryant, D. A. (2002) Insertional inactivation of the *menG* gene, encoding 2-phytyl-1,4-naphthoquinone methyltransferase of Synechocystis sp. PCC 6803 results in the incorporation of 2-phytyl-1,4-naphthoquinone into the A_1 site and alteration of the equilibrium constant between A_1 and F_X in Photosystem I. *Biochemistry 41*, 394–405.
36. Srinivasan, N., and Golbeck, J. H. Protein-cofactor interactions in bioenergetic complexex: Role of A_{1A} and A_{1B} phylloquinones in Photosystem I. *Biochim. Biophys. Acta*, submitted.
37. Pushkar, Y. N., Zech, S. G., Stehlik, D., Brown, S., van der Est, A., and Zimmermann, H. (2002) Orientation and protein-cofactor interactions of monosubstituted *n*-alkyl naphthoquinones in the A_1 binding site of Photosystem I. *J. Phys. Chem. B 106*, 12052–12058.
38. Semenov, A. Y., Vassiliev, I. R., van der Est, A., Mamedov, M. D., Zybailov, B., Shen, G., Stehlik, D., Diner, B. A., Chitnis, P. R., and Golbeck, J. H. (2000) Recruitment of a foreign quinone into the A_1 site of Photosystem I. Altered kinetics of electron transfer in phylloquinone biosynthetic pathway mutants studied by time-resolved optical, EPR, and electrometric techniques. *J. Biol. Chem. 275*, 23429–23438.
39. Sakuragi, Y., Zybailov, B., Shen, G., Bryant, D. A., Golbeck, J. H., Diner, B. A., Karygina, I., Pushkar, Y., and Stehlik, D. (2005) Recruitment of a foreign quinone into the A_1 site of Photosystem I. Characterization of a *menB rubA* double deletion mutant in *Synechococcus* sp. PCC 7002 devoid of F_X, F_A, and F_B and containing plastoquinone or exchanged 9,10-anthraquinone. *J. Biol. Chem. 280*, 12371–12381.
40. Johnson, T. W., Shen, G., Zybailov, B., Kolling, D., Reategui, R., Beauparlant, S., Vassiliev, I. R., Bryant, D. A., Jones, A. D., Golbeck, J. H., and Chitnis, P. R. (2000) Recruitment of a foreign quinone into the A_1 site of Photosystem I. I. Genetic and physiological characterization of phylloquinone biosynthetic pathway mutants in *Synechocystis* sp. PCC 6803. *J. Biol. Chem. 275*, 8523–8530.
41. Zybailov, B., van der Est, A., Zech, S. G., Teutloff, C., Johnson, T. W., Shen, G., Bittl, R., Stehlik, D., Chitnis, P. R., and Golbeck, J. H. (2000) Recruitment of a foreign quinone into the A_1 site of Photosystem I. II. Structural and functional characterization of phylloquinone biosynthetic pathway mutants by electron paramagnetic resonance and electron-nuclear double resonance spectroscopy. *J. Biol. Chem. 275*, 8531–8539.
42. Johnson, T. W., Zybailov, B., Jones, A. D., Bittl, R., Zech, S., Stehlik, D., Golbeck, J. H., and Chitnis, P. (2001) Recruitment of a foreign quinone into the A_1 site of Photosystem I. In vivo replacement of plastoquinone-9 by media-supplemented naphthoquinones in phylloquinone biosynthetic pathway mutants of *Synechocystis* sp. PCC 6803. *J. Biol. Chem. 276*, 31512–31521.
43. Biggins, J., and Mathis, P. (1988) Functional role of vitamin K_1 in Photosystem I of the cyanobacterium *Synechocystis* 6803. *Biochemistry 27*, 1494–1500.
44. Sieckman, I., van der Est, A., Bottin, H., Setif, P., and Stehlik, D. (1991) Nanosecond electron transfer kinetics in Photosystem I following substitution of quinones for vitamin K_1 as studied by time resolved EPR. *FEBS Lett. 284*, 98–102.
45. van der Est, A., Sieckmann, I., Lubitz, W., and Stehlik, D. (1995) Differences in the binding of the quinone acceptor in Photosystem I and reaction centers of *Rhodobacter Sphaeroides*-R26 studied with transient EPR spectroscopy. *Chem. Phys. 194*, 349–360.
46. Pushkar, Y. N., Karyagina, I., Stehlik, D., Brown, S., and van der Est, A. (2005) Recruitment of a foreign quinone into the A_1 site of Photosystem I Consecutive forward electron transfer from A_0 to A_1 to F_X with anthraquinone in the A_1 site as studied by transient EPR. *J. Biol. Chem. 280*, 12382–12390.
47. Klughammer, C., and Pace, R. J. (1997) Photoreduction of the secondary Photosystem I electron acceptor vitamin K_1 in intact spinach chloroplasts and cyanobacteria *in vivo*. *Biochim. Biophys. Acta 1318*, 133–144.

BI802340S